THE JOURNAL OF PHYSICAL CHEMISTRY B LETTERS

2005, *109,* 5398−5402
Published on Web 03/08/2005

Conjugated Thiol Linker for Enhanced Electrical Conduction of Gold−Molecule Contacts

Alexei V. Tivanski,[†] Yufan He,[‡] Eric Borguet,[‡] Haiying Liu,[§] Gilbert C. Walker,*[,#] and David H. Waldeck*[,†]

Department of Chemistry, University of Pittsburgh, Pittsburgh, Pennsylvania 15260, Department of Chemistry, Temple University, Philadelphia, Pennsylvania 19122, Department of Chemistry, Michigan Technological University, Houghton, Michigan 49931, and Department of Chemistry, University of Toronto, Toronto, Ontario, M5S 3H6 Canada

Received: January 3, 2005; In Final Form: February 19, 2005

Single-molecule electrical conduction studies are used to evaluate how the molecular linking unit influences the tunneling efficiency in metal−molecule−metal (m-M-m) junctions. This work uses conducting-probe atomic force microscopy (CP-AFM) to compare the molecular conduction of two π-bonded molecules: one with a single thiol linker, and another with a conjugated double thiol linker at both ends of the molecules. The results demonstrate that the molecule with conjugated double thiol linkers displays higher conduction in gold−molecule−gold junctions than nonconjugated single thiol−gold contacts.

Introduction

In recent years, improving the electrical conduction of molecular wires by using conjugated molecules has been a major focus in molecular electronics. However, the conduction of the molecule can become very large, so the metal−molecule−metal (m-M-m) contacts can dominate the response. Recent experimental[1−9] and theoretical[10−15] work has demonstrated the importance of metal−molecule contacts to the efficiency of charge transfer through m-M-m junctions. Particularly, for alkanethiol-based junctions, metal−molecule contact resistance decreased up to 2 orders of magnitude when chemically bonded contacts were used instead of nonbonded (mechanical) contacts.[1] Unlike electrical conduction studies on saturated molecules, fewer experimental studies address how the contacts effect conduction through conjugated molecular systems. This work demonstrates that the efficiency of charge transport through π-bonded molecules forming m-M-m junctions with thiol linking units between the metals and the molecule can be improved by using conjugated double thiol linkers at both ends of the molecule. This knowledge should be useful for the design and fabrication of more-efficient electrical and optical devices with potential use in molecular electronics.

This work compares electrical conduction measurements for gold−molecule−gold tunnel junctions containing two different types of gold−molecule contacts: single gold−sulfur−Ar−sulfur−gold and double gold−S_2C−Ar−CS_2−gold contacts at both ends of the molecule, where Ar is a biphenyl moiety. The gold−S_2C−Ar−CS_2−gold contacts are postulated to provide two points of contact with each gold electrode and better conjugation to the molecule's π-system than the single gold−sulfur−Ar−sulfur−gold contact. The junctions are formed using conducting-probe atomic force microscopy (CP-AFM),[16] in which a platinum-coated AFM probe serves as the contact to the gold nanoparticle electrode and the other electrode is a gold substrate on which the conducting molecules have been assembled (see Chart 1A). Measurements were performed on samples containing isolated conducting molecules in self-assembled monolayers (SAMs) of nonconductive molecules that were prepared using an insertion process.[17] Conduction measurements were performed on single molecules to avoid the uncertainty in the exact number of conducting molecules forming a junction. Good electrical contact between the conductive AFM probe and the conducting molecule was achieved by covalently attaching gold nanoparticles to the exposed sulfur groups of the molecules.[2] The two molecules compared in this study are biphenyl-4,4′-dithiol (**1**) and biphenyl-4,4′-dicarbodithioic acid (**2**) (see Chart 1B).

Experimental Section

SAM Preparation. All 1-hexanethiol (C_6, Sigma−Aldrich Corp., St. Louis, MO) SAMs were formed by exposing the freshly prepared Au(111) facet of a single crystalline bead[18] to 1 mM C_6 solution in ethanol for ∼2 days and then were rinsed in ethanol and dried in a stream of nitrogen gas. The biphenyl-4,4′-dicarbodithioic acid was synthesized according to a method developed by Gotthardt and co-workers.[19] ^{1}H NMR (300 MHz, NaOD, D_2O): δ 7.65 (d, J = 9 Hz, 4H), 7.12 (d, J = 9 Hz, 4H). m/z (%): 306 (M^+, 28%), 273 (66%), 241 (100%), 196 (56%), 152 (58%), 120 (32%), 76 (20%). Briefly, the compound was dissolved in a 0.1 M NaOH water/ethanol (1:1, v/v) solution at a concentration of 0.5 mM. The gold substrate with the C_6 SAM was then immersed into the solution for 60 min to form mixed monolayers using the insertion process.[17] After assembly, the sample was rinsed with water, and then with ethanol, and subsequently dried in a stream of nitrogen gas.

The thioacetic acid S-(4′-acetylsulfanyl-biphenyl-4-yl) ester was synthesized according to procedures described elsewhere.[20,21] ^{1}H NMR (300 MHz, $CDCl_3$): δ 2.54 (s, 6H), 7.70

* Authors to whom correspondence should be addressed. E-mail addresses: gwalker@chem.utoronto.ca, dave@pitt.edu.
[†] University of Pittsburgh.
[‡] Temple University.
[§] Michigan Technological University.
[#] University of Toronto.

10.1021/jp050022d CCC: $30.25

CHART 1. (A) Schematic of the CP-AFM Experiment, and (B) Molecular Structures of the Molecules That Are Compared in This Study.

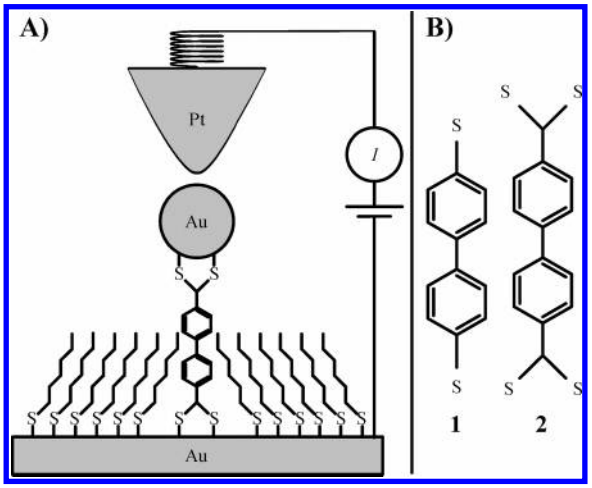

(d, $J = 9$ Hz, 4H), 7.57 (d, $J = 9$ Hz, 4H). *m/z*: (%) 302 (M^+, 100%), 260 (60%), 218 (98%), 184 (16%). The compound was dissolved in a freshly distilled CH_2Cl_2 solution (Sigma−Aldrich Corp., St. Louis, MO) at a concentration of 1 mM. The gold bead with a C_6 SAM was exposed to this solution for 75 min to form mixed monolayers. After assembly, the sample was rinsed in distilled CH_2Cl_2 and then exposed to a 0.1 M H_2SO_4 solution for 20 min to remove the acetate and deprotect the thiol groups on the outer surface of the SAM. This procedure was followed by rinsing in distilled CH_2Cl_2 solution and drying in a stream of nitrogen gas.

The gold beads with inserted molecules were incubated overnight in a gold nanoparticle solution (Ted Pella, Inc., Redding, CA) with a nanoparticle core diameter of ∼5 nm, followed by rinsing in water and ethanol, and then drying in a stream of nitrogen gas. The gold nanoparticles were stabilized with citrate ligand. All preparations were performed at room temperature, and all samples were used within 2 days of preparation.

Scanning Probe Measurements. The CP-AFM measurements were performed using a commercial contact-mode AFM system (Molecular Force Probe, Asylum Research, Santa Barbara, CA) that was modified in Pittsburgh for conducting-probe experiments. Different fixed-tip biases were applied, and currents through the junctions were measured (using a pico-ammeter, Chem-Clamp, Dagan Corp., Minneapolis, MN) as a function of vertical piezo displacement simultaneously with independent force detection between the tip and the sample. The sample was not scanned in horizontal directions; instead, the AFM tip was allowed to thermally drift over the sample surface. Currents were measured over different gold nanoparticles for different contact forces and were averaged over the number of repeated measurements to obtain averaged force-dependent current−voltage ($I-V$) characteristics of the junction. The experimental error is primarily dominated by uncertainty in the tip-to-gold-nanoparticle contact. Because the tip drifts over the surface, variations in the compressing force may cause fluctuations in the measured current. In addition, variations in the biphenyl torsion, arising from environmental changes, could modify the measured conductance. All experiments reported here were performed in an insulating bicyclohexyl solvent (99.0%, Fluka, Switzerland) to reduce water contamination and decrease the adhesion forces between the probe and the sample. Platinum-coated V-shaped silicon cantilevers (MikroMasch, Estonia) with

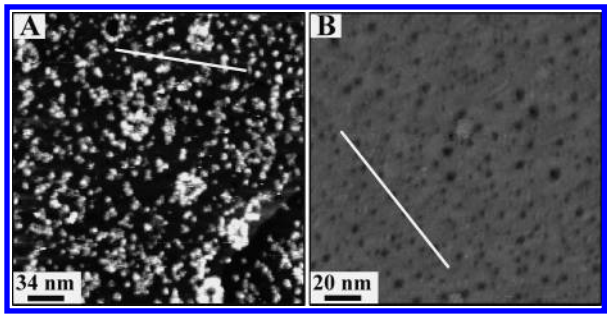

Figure 1. (A) Constant-current scanning tunneling microscopy (STM) image of biphenyl-4,4′-dicarbodithioic acid (**2**) inserted into a C_6 self-assembled monolayer (SAM) with gold nanoparticles (bright spots) attached to the thiol groups (270 nm × 270 nm). (B) STM image of a pure C_6 SAM (160 nm × 160 nm).

force constants of ∼0.8 N/m and tip radii of curvature of ∼25 nm were used in this work. The cantilevers were cleaned in Piranha solution (1:3 of 30% H_2O_2/98% H_2SO_4) for 5 min, rinsed in distilled water (purified to 18 MΩ cm) for 1 min, then soaked in hydrofluoric acid (HF) for 20 s, and finally rinsed again in distilled water for 1 min, followed by drying under vacuum. *Caution! Piranha solution is a very strong oxidant and is extremely dangerous to work with; gloves, goggles, and a face shield should be worn.*

Scanning tunneling microscopy (STM) images were obtained with a PicoScan STM system (Molecular Imaging Inc., Tempe, AZ) that was operating in air. A tunneling current of 10 pA and a tip bias of 0.8 V were used.

Results and Discussion

Evidence for Single-Molecule Measurements. Single-molecule measurements were achieved by inserting a small number of conductive molecules into a SAM of 1-hexanethiol (C_6) on gold. Several steps were taken to ensure that single molecules (or, at most, a few molecules) were probed in each experiment. First, the physical properties of assemblies at different preparation stages were characterized using STM. Figure 1A shows a constant-current STM image of a C_6 SAM with inserted molecules of **2** that were exposed to a gold nanoparticle solution. Sizes of the observed bright spots compare reasonably well to the core diameter of a gold nanoparticle (∼5 nm), implying that they correspond to immobilized nanoparticles (for a cross section, corresponding to the white lines in Figure 1, see Figure 1SM in the Supporting Information). In contrast, the exposure of a pure C_6 SAM to the same solution displays no bright spots (see Figure 1B), confirming that the gold nanoparticles attach only to the inserted conductive molecules.

Second, the solution concentrations and incubation times for insertion of **1** and **2** into SAMs were adjusted so that 10%−15% of the force plots correspond to gold nanoparticles. The majority (>85%) of the data correspond to measurements on nonconducting C_6 molecules with the conducting AFM probe thermally drifting over the sample surface. In the approximation that the nanoparticle distribution is random and the contact area is 5.4 nm^2 (5 nN of compressing force and a tip radius on C_6 of 25 nm), this condition corresponds to <0.2% conducting molecules in the film. These low concentrations were used to minimize the probability of having several molecules form a junction to the nanoparticle. Particularly, for molecule **2**, electrostatic repulsion between negatively charged conducting molecules is likely to inhibit them from coming into close proximity with each other.

Because the particles are not necessarily distributed randomly, a statistical analysis of the measurements was implemented.

Under the loading force of 5 nN used in this study, the contact area between the gold nanoparticle and sample was estimated to be 1.8 nm^2, using a Hertzian elastic contact model.[22] Using a molecular cross section of 0.3 nm^2, the contact area estimate implies that, at most, six conducting molecules could contact a single particle. If the number of conducting molecules is distributed on different nanoparticles according to the Poisson distribution,[23] the current magnitudes should appear in clusters, corresponding to the number of conducting molecules.[2] For a coverage of 0.2% conducting molecules, the probability of two molecules being under a nanoparticle would be $<2 \times 10^{-5}$. Although the distribution is not likely to be random, for the hundreds to thousands of $I-V$ curves collected here, no clustering was observed.

Last, if each nanoparticle binds to multiple conducting molecules, then one might expect fluctuations in the number of contacts to the nanoparticle. For a Poisson distribution, the mean and variance of the distribution should be equal to each other; hence, the variances of the current distributions at different biases should scale linearly with the average current, if there were multiple conducting molecules under each nanoparticle. A statistical analysis shows that the variance in the measured current distributions at different biases does not change with the average current (with 95% confidence; see Figure 2SM in the Supporting Information), indicating that the number of molecules contacting nanoparticles remains the same throughout repeated measurements.

Because the sample preparation conditions are likely to yield single contacting molecules per site and it is unlikely that a fixed, large number would occur, we conclude that single-molecule measurements were achieved.

Comparison of Conduction in 1 and 2. Electrical conduction measurements were performed using CP-AFM at different applied tip biases, so that the current through the junction could be measured as a function of tip−sample separation simultaneously with independent detection of the force between the tip and the sample. Force-dependent $I-V$ characteristics of the junction were obtained by averaging over a thousand repeated measurements under different tip biases within a bias range of ±1 V. Higher biases were not applied, because of the increased possibility of chemically modifying the molecule.

Control CP-AFM measurements over a pure C_6 SAM (no conducting molecules present) show that at least 7 nN of loading force, with which the cantilever pushes the probe into the sample, is required to make sufficient electrical contact and cause observable currents of 10 pA or larger. Experiments were performed in bicyclohexyl solvent. The linear portions of the $I-V$ curves (within a bias range of ±0.2 V) were fit to straight lines, and the determined slopes were used to define force-dependent junction resistances. Figure 2 shows a log−log plot of the junction resistance versus the loading force. Possible factors that can change the observed junction resistances under applied loading force include (a) a change in the contact area and the tunneling distance, arising from film compression between the AFM tip and the sample; and (b) intrachain and interchain order of the molecular film.[24] Measurements over a C_6 monolayer with incubation in the gold nanoparticles solution (no conducting molecules) produced similar force-dependent junction resistances, confirming that the gold nanoparticles only attach when the conductive molecules **1** and **2** are inserted.

Figure 3 shows the averaged single-molecule $I-V$ characteristics for **1** (denoted by the symbol "×") and **2** (denoted by the symbol "●") inserted into a C_6 SAM in bicyclohexyl solvent

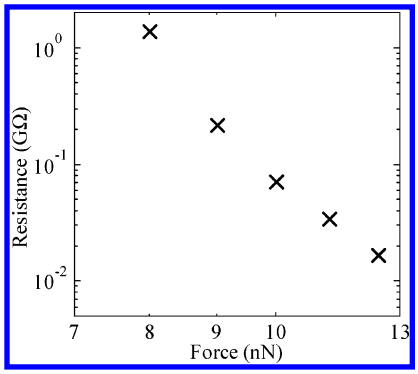

Figure 2. Log−log plot of junction resistance versus loading force for the pure C_6 SAM.

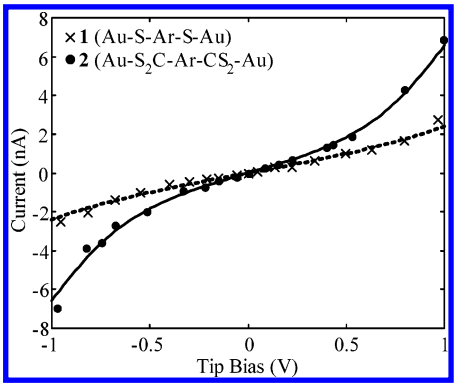

Figure 3. Current−voltage ($I-V$) curves for molecules **1** and **2**; the current is shown as a function of the applied tip bias under a loading force of 5nN. Curves are fits to eq 1 for (×) Au−S−Ar−S−Au and (●) Au−S_2C−Ar−CS_2−Au.

under a fixed loading force of 5 nN. Each data symbol shown in Figure 3 represents the mean value of current for a series of repeated measurements on different gold nanoparticles under a particular tip bias. The standard deviation of the current found in different measurements is similar, or smaller, to the size of the symbol. The $I-V$ characteristics of the conducting molecules were collected under a loading force of 5 nN, to eliminate any direct contribution through the C_6 SAM to the observed electrical current. For an applied loading force of 5 nN, no measurable currents (less than several picoamperes) within a bias range of ±1 V on the pure C_6 monolayer were observed. However, a nonzero loading force was still required to make good electrical contact between the conductive probe and gold nanoparticles and to obtain reproducible measurements. The symmetrical $I-V$ dependences for both bias polarities confirm the formation of good electrical contacts between the molecules and both gold electrodes.

To quantify these results, the $I-V$ curves are compared to the Simmons model for nonresonant tunneling through a metal−insulator−metal junction,[25−27] in which the temperature-independent current I (given in amperes) is defined by

$$I = \left(\frac{e\sigma}{4\pi^2\hbar s^2}\right)\left\{\left(\Phi - \frac{eV}{2}\right)\exp\left[-\frac{2(2m_e)^{1/2}}{\hbar}\alpha\left(\Phi - \frac{eV}{2}\right)^{1/2}s\right] - \left(\Phi + \frac{eV}{2}\right)\exp\left[-\frac{2(2m_e)^{1/2}}{\hbar}\alpha\left(\Phi + \frac{eV}{2}\right)^{1/2}s\right]\right\} \quad (1)$$

where m_e is the electron mass, σ the cross-sectional area of the molecule, s the length of the tunneling barrier, Φ the barrier height (relative to the Fermi level of the gold), and V the applied tip bias. The unitless parameter α is 1 if the approximation of

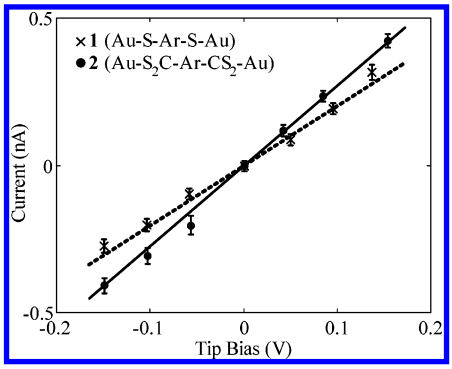

Figure 4. Current−voltage ($I-V$) curves in the ohmic range, showing linear fits for (×) Au−S−Ar−S−Au and (●) Au−S_2C−Ar−CS_2−Au; the current is shown as a function of the applied tip bias under a loading force of 5nN.

an electron tunneling through a rectangular barrier model applies. Deviations from this simple model are manifest as $\alpha \neq 1$ and can arise from a nonrectangular shape of the barrier and/or an effective mass ($m^* = m_e\alpha^2$) for the tunneling electrons through the junction.[27] The lengths of the potential barriers for molecules **1** (s = 1.1 nm) and **2** (s = 1.3 nm) were estimated from molecular lengths that were obtained from semiempirical calculations using the PM3 method. In a corresponding way, the cross-sectional area of the molecules, 0.3 nm^2 was estimated.

The molecular $I-V$ curves for **1** and **2** were fit using eq 1, by adjusting the two parameters Φ and α. These fits are shown by the dotted and solid lines in Figure 3. The best-fit curves have parameter values of $\Phi = 1.35 \pm 0.03$ eV and $\alpha = 0.59 \pm 0.02$ for the Au−S−Ar−S−Au junction and $\Phi = 0.59 \pm 0.02$ eV and $\alpha = 0.66 \pm 0.01$ for the Au−S_2C−Ar−CS_2−Au junction. If the value for α is interpreted in terms of an effective mass for the tunneling electrons, then $m^* = 0.35m_e$ for **1** and $m^* = 0.44m_e$ for **2**. As expected, the potential barriers observed here are smaller than those found for alkanethiol SAMs[27] of the same length.

These results demonstrate enhanced electrical conduction for the junctions involving molecule **2** over that for molecule **1**. Specifically, the tunneling barrier height was ∼0.8 eV smaller and the magnitude of the current for **2** was higher than that of **1**. This latter result is especially noteworthy, because the tunneling length for **2** is ∼0.2 nm larger than that for **1** (because of the presence of two extra C−C bonds), and one would expect the opposite trend.[9]

The observed $I-V$ characteristics were linear within the bias range of ±0.15 V. Figure 4 shows the averaged single-molecule $I-V$ characteristics in the ohmic range of applied tip biases for **1** (denoted by "×") and **2** (denoted by "●") inserted into a C_6 SAM in bicyclohexyl solvent under a fixed loading force of 5 nN. Each data symbol shown in Figure 4 represents the mean value of current for a series of repeated measurements on the different gold nanoparticles under a particular tip bias (error bars represent the standard deviation of the mean). Ohmic dependences observed in the $I-V$ curves are consistent with the Simmons model in the low-bias region[25−27] for nonresonant tunneling through a m-M-m interface. The linear portions of the $I-V$ curves were fit by straight lines, and the obtained slopes were used to determine junction resistances. These fits are shown by the dotted and solid lines in Figure 4 for molecules **1** and **2**, respectively. From the fit, the junction resistances for molecules **1** and **2** were 0.5 ± 0.03 and 0.37 ± 0.02 GΩ, respectively. As expected, these resistance values are smaller than that found for the single-molecule resistance of the similarly long octanedithiol (∼0.8 GΩ),[2] which has no conjugation.

The smaller observed resistances for the junction involving molecule **2** would not be expected, if only molecular lengths were relevant to the electrical conduction. This can be observed from the Simmons model in the low-bias regime for the nonresonant direct tunneling mechanism,[28] in which the junction resistance is predicted to scale exponentially with the length of the tunneling barrier (s). In particular, $R = R_0 s \exp(\beta s)$, where R_0 is a contact resistance and β is a tunneling decay coefficient:

$$\beta = \frac{2(2m_e)^{1/2}}{\hbar}\alpha\sqrt{\Phi} \qquad (2)$$

Using the values for Φ and α that were obtained from the fits in Figure 3, the tunneling decay coefficients are 7 nm^{-1} for **1** and 5 nm^{-1} for **2**. With these parameters, the resistance of a hypothetical molecule **1** with the length of molecule **2** (0.2 nm longer) can be computed and is predicted to be 2.5 GΩ. In fact, the observed resistance for the junction involving molecule **2** is smaller than that of the shorter molecule **1**. The explanation for the improved conductance of **2** must lie with better overlap of the electronic wave functions of the molecule and substrate for the conjugated thiol linker of **2**, providing smaller contact resistance and/or a smaller tunneling decay coefficient.

By modeling conducting molecules as cylinders with a diameter of 0.6 nm and a length s for the width of the tunneling barrier, the molecular resistivities can be estimated from the measured junction resistances. Molecules **1** and **2** display resistivities of 12.9 and 8 Ω cm, respectively. These values are ∼1 order of magnitude smaller than the intrinsic resistivity of bulk germanium (∼65 Ω cm).

Conclusions

These measurements show enhanced conduction for the junctions involving biphenyl-4,4′-dicarbodithioic acid (**2**) over that for biphenyl-4,4′-dithiol (**1**). In particular, the magnitude of the current is higher for **2**, as compared to **1**, and the tunneling barriers that are extracted from the $I-V$ curves are smaller. This result is especially significant because the tunneling length for **2** is larger than that for **1**, and, based on the difference in tunneling length, one would expect the opposite order. Characterization of the contacts implies that only one conducting molecule binds to a gold nanoparticle, so that the smaller tunneling barrier must lie with the difference in overlap of the electronic wave functions of the substrate and the molecules. In summary, this work demonstrates that a conjugated molecule with a double thiol linker on both sides is a more-conductive contact in gold−molecule−gold junctions than a single thiol linker on both sides.

Acknowledgment. D.H.W. acknowledges NSF (NER-0102912); G.C.W. acknowledges NSF (CHE-0404579), ARO (W911NF-04-100191), and ONR (N00014-02-1-0327); and E.B. acknowledges NSF (CHE 0303098) for financial support.

Supporting Information Available: Figure 1SM shows cross sections corresponding to the white lines in Figure 1 (PDF). Figure 2SM shows that variances of the current distributions do not significantly change with the average values of the current (PDF). STM images in Figure 3SM are of a SAM of C_6 alkanethiol with the conducting molecule **2** inserted; this image contains ∼168 000 alkanethiol molecules and 220−260 conducting molecules, for a concentration of 0.13%−0.15%. This material is available free of charge via the Internet at http://pubs.acs.org.

References and Notes

(1) Cui, X. D.; Zarate, X.; Tomfohr, J.; Sankey, O. F.; Primak, A.; Moore, A. L.; Moore, T. A.; Gust, D.; Harris, G.; Lindsay, S. M. *Nanotechnology* **2002**, *13*, 5.

(2) Cui, X. D.; Primak, A.; Zarate, X.; Tomfohr, J.; Sankey, O. F.; Moore, A. L.; Moore, T. A.; Gust, D.; Nagahara, L. A.; Lindsay, S. M. *J. Phys. Chem. B* **2002**, *106*, 8609.

(3) Zhou, C.; Deshpande, M. R.; Reed, M. A.; Jones, L., II; Tour, J. M. *Appl. Phys. Lett.* **1997**, *71*, 611.

(4) Reed, M. A.; Zhou, C.; Muller, C. J.; Burgin, T. P.; Tour, J. M. *Science* **1997**, *278*, 252.

(5) Bumm, L. A.; Arnold, J. J.; Dunbar, T. D.; Allara, D. L.; Weiss, P. S. *J. Phys. Chem. B* **1999**, *103*, 8122.

(6) Beebe, J. M.; Engelkes, V. B.; Miller, L. L.; Frisbie, C. D. *J. Am. Chem. Soc.* **2002**, *124*, 11268.

(7) Fan, F. F.; Yang, J.; Cai, L.; Price, D. W., Jr.; Dirk, S. M.; Kosynkin, D. V.; Yao, Y.; Rawlett, A. M.; Tour, J. M.; Bard, A. J. *J. Am. Chem. Soc.* **2002**, *124*, 5550.

(8) Kushmerick, J. G.; Holt, D. B.; Pollack, S. K.; Ratner, M. A.; Yang, J. C.; Schull, T. L.; Naciri, J.; Moore, M. H.; Shashidar, R. *J. Am. Chem. Soc.* **2002**, *124*, 10654.

(9) Wold, D. J.; Haag, R.; Rampi, M. A.; Frisbie, C. D. *J. Phys. Chem. B* **2002**, *106*, 2813.

(10) Yaliraki, S. N.; Kemp, M.; Ratner, M. A. *J. Am. Chem. Soc.* **1999**, *121*, 3428.

(11) Xue, Y.; Datta, S.; Ratner, M. A. *J. Chem. Phys.* **2001**, *115*, 4292.

(12) Conwell, E. M.; Wu, M. W. *Appl. Phys. Lett.* **1997**, *70*, 1867.

(13) Samanta, M. P.; Tian, W.; Datta, S.; Henderson, J. I.; Kubiak, C. P. *Phys. Rev. B* **1996**, *53*, 7626.

(14) Datta, S.; Tian, W.; Hong, S.; Reifenberger, R.; Henderson, J. I.; Kubiak, C. P. *Phys. Rev. Lett.* **1997**, *79*, 2530.

(15) Bussac, M. N.; Michoud, D.; Zuppiroli, L. *Phys. Rev. Lett.* **1998**, *81*, 1678.

(16) Tivanski, A. V.; Bemis, J. E.; Akhremitchev, B. B.; Liu, H.; Walker, G. C. *Langmuir* **2003**, *19*, 1929.

(17) Cygan, M. T.; Dunbar, T. D.; Arnold, J. J.; Bumm, L. A.; Shedlock, N. F.; Burgin, T. P.; Jones, L.; Allara, D. L.; Tour, J. M.; Weiss, P. S. *J. Am. Chem. Soc.* **1998**, *120*, 2721.

(18) Clavilier, J. F.; Guinet, G.; Durand, R. *J. Electroanal. Chem.* **1980**, *107*, 205.

(19) Gotthardt, H.; Pflaumbaum, W.; Gutowski, P. *Chem. Ber.* **1988**, *121*, 313.

(20) Alov, M. N.; Novikov, S. E.; Kobylinskii, D. B.; Moskvichev, Y. A.; Kryukova, G. G.; Yasinskii, O. A.; Budanov, N. A. *Russ. J. Org. Chem.* **1998**, *34*, 1160.

(21) Hendrik Ehlich, A. S.; Schmidbaur, H. *Inorg. Chem.* **2002**, *41*, 3721.

(22) Weihs, T. P.; Nawaz, Z.; Jarvis, S. P.; Pethica, J. B. *Appl. Phys. Lett.* **1991**, *59*, 3536.

(23) Thomas, J. B. *An Introduction to Applied Probability and Random Processes*; Wiley: New York, 1971.

(24) Tivanski, A. V.; Walker, G. C. submitted for publication.

(25) Sze, S. M. *Physics of Semiconductor Devices*; Wiley: New York, 1981.

(26) Simmons, J. H. *J. Appl. Phys.* **1963**, *281*, 1793.

(27) Wang, W.; Lee, T.; Reed, M. A. *Phys. Rev. B* **2003**, *68*, 035416.

(28) Ratner, M. A.; Davis, B.; Kemp, M.; Mujica, V.; Roitberg, A.; Yaliraki, S. *Ann. N.Y. Acad. Sci.* **1998**, 852.